1572 *Inorg. Chem.* **1994,** *33,* 1572–1574

$[Pt_2(\mu\text{-}S)_2(PPh_3)_4]$ as a Metalloligand toward Main-Group Lewis Acids. The First Square-Pyramidal Structure of an Indium(III) Complex Adduct in $(PPh_3)_4Pt_2(\mu_3\text{-}S)_2InCl_3$ and Tetrahedral Gallium(III) in the Ion Pair $[(PPh_3)_4Pt_2(\mu_3\text{-}S)_2GaCl_2][GaCl_4]$

Meisheng Zhou,* Yan Xu, Choon-Fui Lam, Pak-Hing Leung, Lip-Lin Koh, K. F. Mok, and T. S. Andy Hor*

Department of Chemistry, Faculty of Science, National University of Singapore, Kent Ridge, Singapore 0511

Received October 6, 1993

Introduction

The ability of $Pt_2(\mu\text{-}S)_2(PPh_3)_4$ (**1**) to function as a bidentate ligand toward metals is the subject of our recent research.[1] The isolation of adduct complexes between compound **1** and Tl(I)[2] and Pb(II)[3] demonstrates that this metalloligand can support some unusual geometries of the *p*-block metals (hereafter known as "heterometal" (M)) (e.g. V-shaped Tl(I)[2]) and that they are very dependent on the associated anions. In our continuing search for novel geometries of the heterometal in the environment of **1**, we have extended our study to compare the complexes formed upon the reactions of compound **1** with $GaCl_3$ and $InCl_3$. Among the few structurally characterized adducts of GaX_3 in the literature are $[GaCl_2(monoglyme)][GaCl_4]$ (octahedral (Oh)),[4] $[GaCl_2(bipy)_2][GaCl_4]$ (Oh)[5] $GaX_3(SR_2)$ (X = Cl, Br; R = Me, Et) (tetrahedral),[6] and $GaCl_3(MeBNMe)_3$ (tetrahedral).[7] Structures of InX_3 adducts are predominantly Oh and trigonal bipyramidal (tbp),[8] for example, $InCl_3(OPMe_3)_2(L)$ (L = $OPMe_3$, MeOH, H_2O) (Oh),[9] $InX_3(dmso)_3$ (X = Cl, Br) (Oh),[9] $[InI_2(dmso)_3][InCl_4]$ (Oh),[10] $InCl_3(bipy)(L)$ (L = H_2O, EtOH) (Oh),[11] $InX_3(SYMe_3)_2$ (X = Cl, Br; Y = P, As) (tbp),[12] $InCl_3[OP(NMe_2)_3]_2$ (tbp),[13] $InCl_3(PPh_3)_2$ (tbp),[14] and the spectroscopically characterized $InX_3(SR_2)_2$ (tbp)[15] and $[InX_2(OP(R)Ph_2)_4][InCl_4]$ (X = Cl, R = Ph; X = Br, R = Me) (Oh).[9] The possibility of halide transfer from the 1/1 adduct to the Lewis acid to give an ion pair makes the structural prediction even more difficult.

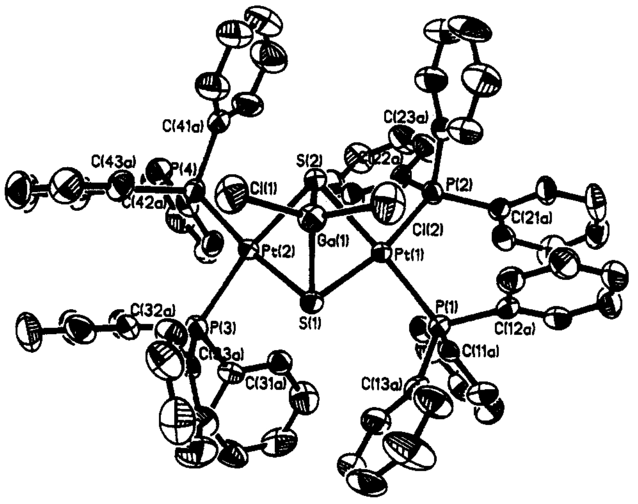

Figure 1. ORTEP plot of the structure of the molecular cation in $[(PPh_3)_4Pt_2(\mu_3\text{-}S)_2GaCl_2][GaCl_4]$ (**2**).

Scheme 1

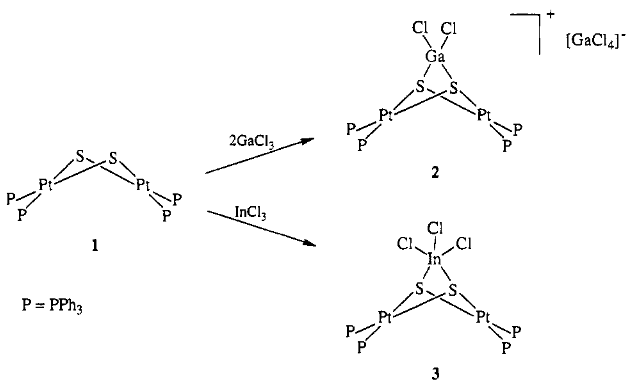

Results and Discussion

Compound **1** reacts readily with a slight excess of $GaCl_3$ in MeOH to give $[(PPh_3)_4Pt_2(\mu_3\text{-}S)_2GaCl_2][GaCl_4]$ (**2**) together with a side product presently unidentified. A stoichiometric excess of $GaCl_3$ is not essential for the formation of **2**. With 1 molar equiv of $InCl_3$, $(PPh_3)_4Pt_2(\mu_3\text{-}S)_2InCl_3$ (**3**) results (see Scheme 1). Molar conductivity measurements indicate **2** to be a 1/1 electrolyte and **3** a nonelectrolyte in CH_2Cl_2. As the solution data could not provide any geometric information, especially on the solid-state structures, X-ray crystallographic diffractometry was carried out on both products. It confirms that both **2** and **3** are adduct complexes formed between **1** and the Lewis acid through the nucleophilic sulfur centers. Compound **3** is 5-coordinated while **2** shows a molecular cation with tetrachlorogallate as the anion. The heterometal is tetrahedral, which is a common geometry for Ga(III), in **2** (Figure 1) and, surprisingly, square-based pyramidal (sbp) in **3** (Figure 2). Selected crystallographic data are given in Table 1, atomic coordinates in Table 2, and bond lengths and angles in Table 3.

Compound **3** is to our knowledge the first crystallographically characterized sbp structure for an adduct complex of InX_3. It also provides the first example of an sbp complex supported by the metalloligand **1**. A recently reported THF adduct, $InCl_3(thf)_2$, is also tbp.[16] The reason for a sbp, rather than tbp, geometry is unclear; however, the acute chelate angle (S(1)–In–S(1a) 70.8(1)°) would possibly raise the energy of a tbp structure to

---

* To whom correspondence should be addressed.

(1) (a) Briant, C. E.; Hor, T. S. A.; Howells, N. D.; Mingos, D. M. P. *J. Chem. Soc., Chem. Commun.* **1983**, 1118. (b) Briant, C. E.; Gilmour, D. I.; Mingos, D. M. P.; Luke, M. A. *J. Chem. Soc., Dalton Trans.* **1985**, 851. (c) Gilmour, D. I.; Luke, M. A.; Mingos, D. M. P. *J. Chem. Soc., Dalton Trans.* **1987**, 335. (d) Briant, C. E.; Hor, T. S. A.; Howells, N. D.; Mingos, D. M. P. *J. Organomet. Chem.* **1983**, *256*, C15.

(2) Zhou, M.; Xu, Y.; Koh, L.-L.; Mok, K. F.; Leung, P.-H.; Hor, T. S. A. *Inorg. Chem.* **1993**, *32*, 1875.

(3) Zhou, M.; Xu, Y.; Lam, C.-F.; Koh, L.-L.; Mok, K. F.; Leung, P.-H.; Hor, T. S. A. *Inorg. Chem.* **1993**, *32*, 4660.

(4) Böck, S.; Nöth, H.; Wietelmann, A. *Z. Naturforsch., B* **1990**, 979.

(5) Restivo, R.; Palenik, G. J. *J. Chem. Soc., Chem. Commun.* **1969**, 867.

(6) Fields, R. O.; Waters, J. H.; Bergendahl, T. J. *Inorg. Chem.* **1971**, *10*, 2808.

(7) Anton, K.; Nöth, H. *Chem. Ber.* **1982**, *115*, 2668.

(8) (a) Carty, A. J.; Tuck, D. G. *Prog. Inorg. Chem.* **1975**, *19*, 243. (b) Gillespie, R. J.; Hargittai, I. *The VSEPR Model of Molecular Geometry*; Allyn and Bacon: Boston, MA, 1991; Chapter 5, pp 103–109. (c) Tuck, D. G. In Wilkinson, G., Gillard, R. D., McCleverty, J. A., Eds.; *Comprehensive Coordination Chemistry*; Pergamon: Oxford, U.K., 1987; Vol. 3, Chapter 25, p 153.

(9) Robinson, W. T.; Wilkins, C. J.; Zhang, Z. *J. Chem. Soc., Dalton Trans.* **1990**, 219.

(10) Einstein, F. W. B. *J. Chem. Soc., Chem. Commun.* **1970**, 1182.

(11) Malyarick, M. A.; Petrosyants, S. P.; Ilyuhin, A. B. *Polyhedron* **1992**, *11*, 1067.

(12) Robinson, W. T.; Wilkins, C. J.; Zhang, Z. *J. Chem. Soc., Dalton Trans.* **1988**, 2187.

(13) Sinha, S. P.; Pakkanen, T. T.; Pakkanen, T. A.; Niinistö, L. *Polyhedron* **1982**, *1*, 355.

(14) Veidis, M. V.; Palenik, G. *J. Chem. Soc., Chem. Commun.* **1969**, 586.

(15) Evans, C. A.; Taylor, M. J. *J. Chem. Soc. A* **1969**, 1343.

(16) Self, M. F.; Mcphail, A. T.; Well, R. L. *Polyhedron* **1993**, *12*, 455.

0020-1669/94/1333-1572$04.50/0

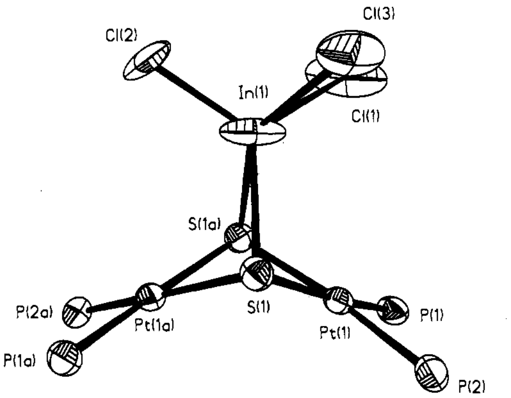

Figure 2. ORTEP plot of the structure of $[(PPh_3)_4Pt_2(\mu_3\text{-}S)_2InCl_3]$ (**3**), (phenyl rings removed for clarity).

Table 1. Crystallographic Data for $[(PPh_3)_4Pt_2(\mu_3\text{-}S)_2GaCl_2][GaCl_4]$ (**2**) and $[(PPh_3)_4Pt_2(\mu_3\text{-}S)_2InCl_3]$ (**3**)

chem formula	$[(PPh_3)_4Pt_2(\mu_3\text{-}S)_2GaCl_2]$-$[GaCl_4]$	$[(PPh_3)_4Pt_2(\mu_3\text{-}S)_2$-$InCl_3]$
fw	1855.5	1724.5
space group	$P2_1/c$ (No. 14)	$C2/c$ (No. 15)
a, Å	14.133(3)	26.273(5)
b, Å	17.399(3)	11.955(2)
c, Å	29.126(6)	21.257(4)
β, deg	94.75(2)	92.96(3)
V, Å^3	7137(3)	6668(3)
Z	4	4
T, K	298	298
λ(Mo Kα), Å	0.710 73	0.710 73
ρ_{obs}, g cm^{-3}	1.722	1.730
ρ_{calc}, g cm^{-3}	1.727	1.718
μ, mm^{-1}	5.068	4.849
no. of obsd rflcns	10 523 ($F > 3.0\sigma(F)$)	4455 ($F > 4.0\sigma(F)$)
$R(F_o)^a$	0.054	0.039
$R_w(F_o)^b$	0.043	0.045

[a] $R = \sum||F_o| - |F_c||/\sum|F_o|$. [b] $R_w = [\sum w(|F_o| - |F_c|)^2/\sum w|F_o|^2]^{1/2}$.

render it unstable. The sulfur and two of the chloride atoms are essentially coplanar (maximum deviation 0.17 Å) and constitute the base of the pyramid. The apical In–Cl(2) bond (2.131(5) Å) is significantly shorter, and presumably stronger, than its basal counterparts (mean 2.597(7) Å). Such large disparity, which is not clearly understood, is not found in $[InCl_5]^{2-}$,[17] which is probably the best known sbp structure for In(III). It remains to be seen that the metathetic/elimination products from InX_3 and Brønsted acids or nucleophiles[18] could form via an sbp intermediate such as **3** and that In–Cl bond cleavage occurs at the basal sites.

The heterometal Ga(1) in the molecular cation of **2** is tetrahedral. The two Ga–S lengths, and Ga–Cl, are essentially identical. Compared to the other complexes identified so far (Table 4), **2** has the shortest M–S lengths and widest S–M–S bite. These contribute to the most acute dihedral angle between the two Pt(II) coordination planes found in **2**.

The precursor of compound **2** is likely an adduct formed between $GaCl_3$ and **1**; chloride migration from this adduct to $GaCl_3$ would then give the cation–anion pair (**2**). Attempts to isolate this intermediate so far have been unsuccessful. However, **3** gives an indication as to the possible structure of the intermediate gallium adduct. Compound **3** is nonconducting in CH_2Cl_2, but upon addition of $InCl_3$, the conductivity increases ≈30 fold (from 0.9 to 30.5 Ω^{-1} cm^2 mol^{-1}), suggesting a chloride-exchange mechanism similar to that proposed for **2**. No strenuous attempt was made to isolate the resultant complex since the chloride-accepting property of $InCl_3$ to give $[InCl_4]^-$ is well-known.[9,10] Compound **2** does not react further with **1** despite the known ability of

Table 2. Atomic Coordinates (×10^4) and Equivalent Isotropic Displacement Coefficients[a] of Selected Non-Hydrogen Atoms (Å^2 × 10^3)

atom	x	y	z	U_{eq}
		(a) $[(PPh_3)_4Pt_2(\mu_3\text{-}S)_2GaCl_2][GaCl_4]$ (**2**)		
Pt(1)	2279(1)	2587(1)	4504(1)	26(1)
Pt(2)	3807(1)	2334(1)	3757(1)	27(1)
Ga(1)	4389(1)	2601(1)	4779(1)	40(1)
S(1)	3524(2)	3376(1)	4265(1)	31(1)
S(2)	3479(2)	1637(1)	4432(1)	32(1)
P(1)	1315(2)	3615(1)	4602(1)	30(1)
P(2)	1283(2)	1628(1)	4717(1)	31(1)
P(3)	4041(2)	3220(1)	3187(1)	34(1)
P(4)	4193(2)	1244(1)	3379(1)	34(1)
Cl(1)	5917(2)	2497(2)	4718(1)	61(1)
Cl(2)	4285(2)	2846(2)	5507(1)	66(1)
Ga(2)	−747(1)	2718(1)	2081(1)	60(1)
Cl(3)	489(2)	3037(2)	1732(1)	66(1)
Cl(4)	−1315(2)	3715(2)	2400(1)	72(1)
Cl(5)	−1860(3)	2251(2)	1610(1)	112(2)
Cl(6)	−294(3)	1863(2)	2598(2)	129(2)
		(b) $[(PPh_3)_4Pt_2(\mu_3\text{-}S)_2InCl_3]$ (**3**)		
Pt(1)	603(1)	2292(1)	2716(1)	42(1)
In(1)	0	−149(1)	2500	92(1)
Cl(1)	538(4)	−884(6)	3515(3)	167(4)
Cl(2)	−694(2)	−1068(5)	2391(5)	148(5)
Cl(3)	620(3)	−1344(5)	1926(3)	112(3)
S(1)	130(1)	1633(1)	1814(1)	45(1)
P(1)	962(1)	2788(2)	3686(1)	54(1)
P(2)	1230(1)	2918(2)	2082(1)	53(1)

[a] Equivalent isotropic U_{eq} defined as one-third of the trace of the orthogonalized $\mathbf{U}_{ij}$ tensor.

Table 3. Selected Bond Distances (Å) and Angles (deg)

(a) $[(PPh_3)_4Pt_2(\mu_3\text{-}S)_2GaCl_2][GaCl_4]$ (**2**)			
Pt(1)–S(1)	2.381(2)	Pt(1)–S(2)	2.390(2)
Pt(2)–S(1)	2.396(2)	Pt(2)–S(2)	2.388(2)
mean Pt–P	2.292(2)	Ga(1)–S(1)	2.291(2)
Ga(1)–S(2)	2.297(2)	Ga(1)–Cl(1)	2.189(3)
Ga(1)–Cl(2)	2.181(3)	Ga(2)–Cl(3)	2.165(3)
Ga(2)–Cl(4)	2.155(3)	Ga(2)–Cl(5)	2.160(4)
Ga(2)–Cl(6)	2.172(5)	Pt(1)···Pt(2)	3.220(1)
S(1)···S(2)	3.066(4)	mean Ga···Pt	3.041(1)
S(1)–Pt(1)–S(2)	80.0(1)	S(1)–Pt(1)–P(1)	92.7(1)
S(2)–Pt(1)–P(2)	88.7(1)	P(1)–Pt(1)–P(2)	98.6(1)
S(1)–Pt(2)–S(2)	79.7(1)	S(1)–Pt(2)–P(3)	88.9(1)
S(2)–Pt(2)–P(4)	92.6(1)	P(3)–Pt(2)–P(4)	98.9(1)
S(1)–Ga(1)–S(2)	83.9(1)	S(1)–Ga(1)–Cl(1)	118.2(1)
S(2)–Ga(1)–Cl(1)	115.1(1)	S(1)–Ga(1)–Cl(2)	116.4(1)
S(2)–Ga(1)–Cl(2)	119.4(1)	Cl(1)–Ga(1)–Cl(2)	104.0(1)
Pt(1)–S(1)–Pt(2)	84.8(1)	Pt(1)–S(2)–Pt(2)	84.8(1)
mean Pt–S–Ga	81.0(1)		
dihedral angle Pt(1)–S(1)–S(2)–Pt(2)	123.1(3)		
(b) $[(PPh_3)_4Pt_2(\mu_3\text{-}S)_2InCl_3]$ (**3**)			
Pt(1)–S(1)	2.366(2)	Pt(1)–S(1a)	2.351(2)
Pt–P(1)	2.300(2)	Pt–P(2)	2.306(2)
In(1)–Cl(1)	2.666(7)	In(1)–Cl(2)	2.131(5)
In(1)–Cl(3)	2.528(7)	In(1)–S(1)	2.614(2)
Pt(1)···Pt(1a)	3.253(2)	S(1)···S(1a)	3.030(2)
mean In···Pt	3.341(3)		
S(1)–Pt(1)–S(1a)	79.9(1)	S(1)–Pt(1)–P(1)	170.5(1)
S(1)–Pt(1)–P(2)	89.7(1)	S(1a)–Pt(1)–P(2)	169.3(1)
S(1a)–Pt(1)–P(1)	90.7(1)	P(1)–Pt(1)–P(2)	99.7(1)
S(1)–In(1)–S(1a)	70.8(1)	Cl(1)–In(1)–Cl(2)	109.4(3)
Cl(1)–In(1)–Cl(3)	82.9(2)	Cl(2)–In(1)–Cl(3)	103.0(3)
Cl(1)–In(1)–S(1)	129.9(2)	Cl(2)–In(1)–S(1)	119.7(2)
Cl(3)–In(1)–S(1)	94.9(2)	Cl(1)–In(1)–S(1a)	84.0(2)
Cl(2)–In(1)–S(1a)	110.2(2)	Cl(3)–In(1)–S(1a)	146.7(2)
dihedral angle Pt(1)–S(1)–S(1a)–Pt(1a)	128.3(2)		

---

(17) Joy, G.; Gaughan, A. P., Jr.; Wharf, I.; Shriver, D. F.; Dougherty, J. P. *Inorg. Chem.* **1975**, *14*, 1795. Brown, D. S.; Einstein, F. W. B.; Tuck, D. G. *Inorg. Chem.* **1969**, *8*, 14.

(18) Healy, M. D.; Laibinis, P. E.; Stupik, P. D.; Barron, A. R. *J. Chem. Soc., Chem. Commun.* **1989**, 359. Day, R. O.; Holmes, R. R. *Inorg. Chem.* **1982**, *21*, 2379.

Table 4. Comparison of Selected Structural Data for $[Pt_2(\mu\text{-}S)(\mu\text{-}SCH_3)(PPh_3)_4][PF_6]$ (**A**), $[(PPh_3)_4Pt_2(\mu_3\text{-}S)_2GaCl_2][GaCl_4]$ (**2**) (**B**), $(PPh_3)_4Pt_2(\mu_3\text{-}S)_2InCl$, (**3**) (**C**), $[(PPh_3)_4Pt_2(\mu_3\text{-}S)_2Tl][PF_6]$ (**D**), $[(PPh_3)_4Pt_2(\mu_3\text{-}S)_2Pb(NO_3)][NO_3]$ (**E**), and $[(PPh_3)_4Pt_2(\mu_3\text{-}S)_2Pb(NO_3)][PF_6]$ (**F**) (M = Heterometal)

complex	S···S, Å	Pt···Pt, Å	M–S, Å	S–M–S, deg	Pt–S–S–Pt (dihedral), deg
A	3.058(8)	3.307(1)			137.8
B	3.066(4)	3.220(1)	2.294(2)	83.9(1)	123.1(3)
C	3.030(2)	3.253(2)	2.614(2)	70.8(1)	128.3(2)
D	3.126(5)	3.293(2)	2.764(3)	68.9(1)	135.7(1)
E	3.060(4)	3.266(2)	2.718(4)	68.5(1)	132.2(1)
F	3.072(3)	3.290(2)	2.704(3)	69.2(1)	133.5(1)

Ga(III) to give octahedral species.[4,5] Steric hindrance is probably responsible.

Comparison of these two structures to the Tl(I),[2] Pb(II),[3] and thiolato[19] complexes reported reveals some common characteristics: (i) **1** as a chelating ligand is rather rigid in terms of its practically constant S···S and Pt···Pt distances. Its ability to stabilize adducts of different geometries relies largely on its variable chelate bites (refer to Table 4). (ii) The largest dihedral angle between the two Pt planes is found in $[Pt_2(\mu\text{-}S)(\mu\text{-}SCH_3)(PPh_3)_4][PF_6]$,[19] in which the sulfur atoms are free from any constraints arising from chelation. On the basis of the limited data available to date (Table 4), this angle appears to depend more on the M–S distances than on the acidity of the heterometal or the ligands on it. The smallest angle (123.1(3)°) is found with the shortest M–S distance (2.294(2) Å) (in **2**) whereas the largest angle (in the mixed-metal complexes) (135.7(1)°) is associated with the longest length (2.764(3) Å) (in the Tl complex). Related to this, the M–S distances also show an inverse relationship compared to the S–M–S chelate angles. These dependencies can be understood on the basis of a sulfur-bicapped triangular plane, Pt_2M, in which the dihedral angle (∠Pt–S···S–Pt) depends on the relative Pt–S and M–S lengths. (iii) The heterometal does not necessarily show its usual geometry. The strongly chelating ability of **1**, coupled with the presence (or absence) of weakly coordinating anions, governs the resultant geometry, which is largely unpredictable. (iv) Despite the presence of ionizable ligands, none of these complexes shows any further Lewis acidity toward **1**. There is also little tendency for coordination expansion of the capping sulfur ligands even in the excess of the Lewis acid.

Experimental Section

All preparations were carried out under dry argon atmosphere and in dry oxygen-free solvents. Routine ^1H and ^{31}P NMR spectra were recorded at 25 °C on a Bruker ACF 300 spectrometer. Conductivities were measured by using a Horiba ES-12 conductivity meter. Elemental analyses were performed by the Microanalytical Laboratory in our department.

$[(PPh_3)_4Pt_2(\mu_3\text{-}S)_2GaCl_2][GaCl_4]$ (2). $GaCl_3$ (0.056 g, 0.318 mmol) was added to a MeOH suspension (50 mL) of $Pt_2S_2(PPh_3)_4$ (0.350 g, 0.233 mmol) and the mixture stirred for 24 h. The resultant cream white suspension was filtered, and the solid obtained was recrystallized from a CH_2Cl_2/hexane mixture to give fine cream white crystals of **2**. The byproduct contained in the orange filtrate was presently unidentified. Yield: 0.146 g (36%). Anal. Calcd: C, 46.59; H, 3.24; Cl, 11.47; P, 6.68; Pt, 21.04; S, 3.46. Found: C, 46.65; H, 3.22; Cl, 10.49; P, 6.63; Pt, 21.58; S, 3.27. ^{31}P NMR ($CDCl_3$): $\delta = 15.79$ ($J(P\text{–}Pt) = 3270$ Hz). Molar conductivity Λ_m (10^{-3} M, CH_2Cl_2): 57.3 Ω^{-1} cm^2 mol^{-1}.

$[(PPh_3)_4Pt_2(\mu_3\text{-}S)_2InCl_3]$ (3). $InCl_3$ (0.025 g, 0.11 mmol) was mixed and stirred with $Pt_2S_2(PPh_3)_4$ (0.170 g, 0.11 mmol) in MeOH (50 mL) for 5 h. The initial orange suspension readily gave way to a bright yellow solution. The solvent was removed under vacuum and the residue crystallized from CH_2Cl_2/hexane to give yellow microcrystals of **3**. Yield: 0.143 g (73%). Anal. Calcd: C, 50.13; H, 3.48; Cl, 6.17; In, 6.66; P, 7.19; Pt, 22.64; S, 3.72. Found: C, 49.64; H, 3.49; Cl, 6.53; In, 6.10; P, 5.58; Pt, 19.60; S, 3.85. ^{31}P NMR ($CDCl_3$): $\delta = 18.99$ ($J(P\text{–}Pt) = 3080$ Hz, $^3J(P\text{–}Pt) = 16$ Hz). Molar conductivity Λ_m (10^{-3} M, CH_2Cl_2): 0.91 Ω^{-1} cm^2 mol^{-1} (cf. $InCl_3$: 0.08 Ω^{-1} cm^2 mol^{-1}). The conductivity increases to 30.5 Ω^{-1} cm^2 mol^{-1} upon addition of 1 molar excess of $InCl_3$. The resultant mixture gives a single ^{31}P resonance at δ 17.18 ppm.

X-ray Crystal Structure Determination. Colorless and yellow prismatic crystals of **2** and **3**, respectively, suitable for a single-crystal X-ray diffractometry were grown by the slow diffusion of hexane into the sample solution in CH_2Cl_2. The crystals used for analysis are of approximate dimensions 0.20 × 0.20 × 0.30 mm for **2** and 0.50 × 0.50 × 0.40 mm for **3**. The unit cell constants were determined by least-squares fits to the setting parameters of 25 and 21 independent reflections for **2** and **3**. Detailed crystallographic data are listed in Table 1. Totals of 16 311 ($2.5° < 2\theta < 55.0°$) independent reflections for **2** and 10 490 ($3.5° < 2\theta < 48.0°$) for **3** were measured by scanning on a Siemens R3m/V four-circle diffractometer with a beam monochromator. The intensity data were reduced and corrected for Lorentz and polarization factors using the applied programs. Semiempirical absorption corrections were applied. The crystal structures were solved by direct methods using the XS program of SHELXTL-PLUS[20] by using a DEC MicroVax-II minicomputer and refined by full-matrix least-squares analysis with the SHELXTL-PC programs on an IBM-compatible 486 PC to give final *R* factors of 0.054 for **2** and 0.039 for **3** and weighted *R* factors of 0.043 for **2** and 0.045 for **3**. All non-hydrogen atoms were refined anisotropically. The hydrogen atoms were placed at calculated positions with fixed isotropic thermal parameters. The three chlorine atoms in **3** are disordered into two sets (Cl(1–3) and Cl(1a–3a)), each having an SOF of 0.5. One set of the chlorines together with half of the molecular cation constitute an asymmetric unit of **3**. Figure 2 shows the molecular cation with one set of the chlorines.

Acknowledgment. The authors acknowledge the National University of Singapore for financial support (Grant RP850030), the technical staff in our department for supporting services, A.-M. Tan for furnishing some experimental data, and Y. P. Leong for assistance in the preparation of the manuscript.

Supplementary Material Available: Details of the X-ray structural analyses for **2** and **3**, including tables of crystallographic data, refined atomic coordinates and isotropic thermal parameters, anisotropic thermal parameters, and bond distances and angles (19 pages). Ordering information is given on any current masthead page. Listings of structure factors for **2** (37 pages) and **3** (12 pages) can be obtained from the corresponding authors.

---

(19) (a) Hor, T. S. A. D.Phil. Thesis, University of Oxford, 1984. (b) Briant, C. E.; Gardner, C. J.; Hor, T. S. A.; Howells, N. D.; Mingos, D. M. P. *J. Chem. Soc., Dalton Trans.* **1984**, 2645.

(20) Siemens Analytical X-Ray Instruments, Inc., Madison, WI, 1989.